27. Wood, S. A., Allen, N. D., Rossant, J., Auerbach, A. & Nagy, A. Non-injection methods for the production of embryonic stem cell-embryo chimaeras. *Nature* **365**, 87–89 (1993).

Supplementary Information accompanies the paper on **www.nature.com/nature**.

Acknowledgements We thank M. Miwa and H. Satake for technical assistance. We also thank S. Sugano for donation of the pEF321-T plasmid; K. Ono and K. Tanaka for histological examination of the brain; M. Tamagawa for instruction in electrocardiogram recording; and S. Nishio, N. Tsunekawa and M. Terai for discussions. Amino acid measurements were carried out with the aid of the Center for Analytical Instruments at the National Institute for Basic Biology. This work was supported in part by Grants-in-aid for Scientific Research from the Ministry of Education, Culture, Sports, Science and Technology of Japan.

Competing interests statement The authors declare that they have no competing financial interests.

Correspondence and requests for materials should be addressed to N.M. (nmizu@rinshoken.or.jp).

An endoribonuclease-prepared siRNA screen in human cells identifies genes essential for cell division

Ralf Kittler[1], Gabriele Putz[1], Laurence Pelletier[1], Ina Poser[1], Anne-Kristin Heninger[1], David Drechsel[1], Steffi Fischer[1], Irena Konstantinova[1], Bianca Habermann[2], Hannes Grabner[1], Marie-Laure Yaspo[3], Heinz Himmelbauer[3], Bernd Korn[4], Karla Neugebauer[1], Maria Teresa Pisabarro[1]* & Frank Buchholz[1]

[1]*Max Planck Institute for Molecular Cell Biology and Genetics, Pfotenhauerstrasse 108, D-01307 Dresden, Germany*
[2]*Scionics Computer Innovation, GmbH, Pfotenhauerstrasse 110, D-01307 Dresden, Germany*
[3]*Max Planck Institute for Molecular Genetics, Ihnestrasse 73, D-14195 Berlin-Dahlem, Germany*
[4]*RZPD-Ressourcenzentrum für Genomforschung, Im Neuenheimer Feld 506, D-69120 Heidelberg, Germany*

* Present address: TU Dresden, Biotechnologisches Zentrum, Tatzberg 47-51, D-01307 Dresden, Germany

RNA interference (RNAi) is an evolutionarily conserved defence mechanism whereby genes are specifically silenced through degradation of messenger RNAs; this process is mediated by homologous double-stranded (ds)RNA molecules[1–4]. In invertebrates, long dsRNAs have been used for genome-wide screens and have provided insights into gene functions[5–8]. Because long dsRNA triggers a nonspecific interferon response in many vertebrates, short interfering (si)RNA or short hairpin (sh)RNAs must be used for these organisms to ensure specific gene silencing[9–11]. Here we report the generation of a genome-scale library of endoribonuclease-prepared short interfering (esi)RNAs[12] from a sequence-verified complementary DNA collection representing 15,497 human genes. We used 5,305 esiRNAs from this library to screen for genes required for cell division in HeLa cells. Using a primary high-throughput cell viability screen followed by a secondary high content videomicroscopy assay, we identified 37 genes required for cell division. These include several splicing factors for which knockdown generates mitotic spindle defects. In addition, a putative nuclear-export terminator was found to speed up cell proliferation and mitotic progression after knockdown. Thus, our study uncovers new aspects of cell division and establishes esiRNA as a versatile approach for genomic RNAi screens in mammalian cells.

We generated a large-scale RNAi library using an alternative approach to previously reported RNAi expression libraries[13–15]. Our approach was based on the processing of long dsRNA by *Escherichia coli* RNaseIII *in vitro* (Fig. 1a). EsiRNAs generate a variety of siRNAs, which are able to efficiently and specifically silence target mRNA; this abolishes the need to identify effective silencers for each mRNA[16–18]. Moreover, this technology, compared with transfection- or viral expression-based approaches, allows far greater control over interfering dsRNAs at the cellular level; low rates of plasmid transfection or variations in virus titres can be problematic for RNAi studies. Because of its simplicity, efficiency and cost-effectiveness (approximately US$4 per gene), esiRNA has advantages for large-scale loss-of-function studies in mammalian cells.

Assuming that genes essential for cell division are likely to present a cell viability phenotype, we used the simple and fast WST-1 assay as an initial screen to identify 275 genes; these genes were then studied in detail by videomicroscopy to allow detailed spatial and temporal visualization of mitosis and cytokinesis (Fig. 1b). We observed severe cell division phenotypes for 37 genes (Table 1 and Supplementary Table 1). Each of these genes was checked for functional annotation in the HARVESTER[19] unification database and in the scientific literature. No functional annotation was found for seven out of the 37 genes, so we can assign a function in cell division to seven previously uncharacterized genes. For example, knockdown of the predicted mRNAs DKFZP564M082 and FLJ30851 resulted in mitotic arrest and severe spindle defects in the cells (Figs 2d and 3g, h). Functional annotations were found for the remaining 30 genes, but seven of these are based on electronic annotation and have not been experimentally verified. Interestingly, 23 genes had previously only been associated with functions other than cell division.

We grouped the 37 observations of cell division phenotypes (http://www.mpi-cbg.de/esiRNA) into three categories: mitotic arrest (Fig. 2b, d and Supplementary Fig. 1), aberrant cytokinesis (Fig. 2g, h) and cell death upon entry into mitosis (Fig. 2i). Nineteen out of 37 esiRNAs that caused mitotic arrest led to cell death after prolonged latency in mitosis. These genes probably stop the cells from progressing further through mitosis and ultimately induce cell death. Six of the 37 mRNA knockdowns caused the cells to die quickly upon entry into mitosis. Therefore, these genes might be directly linked to cell death at the point of entry into mitosis.

Twelve esiRNAs led to an aberrant cytokinesis phenotype, of which ten also displayed a mitotic arrest phenotype. These phenotypes could further be divided into two classes. The knockdown of *ITPR1*, *MFAP1*, *AD024*, *GALNT5*, *CKLFSF4* and KIAA0056 resulted in a cell cleavage defect leading to bi-nucleated cells after mitosis (Fig. 2g). A different cytokinesis phenotype was observed for *SNRPA1*, *SNRPB*, *DHX8*, *SNW1*, FLJ10290, and importin-β (*KPNB1*). With these knockdowns, some of the cells become round (as normally observed for cells entering mitosis) but exit mitosis some time later, without any sign of cell division. These cells then contain only one nucleus, which has a disorganized appearance; for example, substructures such as the nucleoli are not visible (Fig. 2h). For *DHX8* and *SNW1*, we also observed a cytokinesis defect that led to the formation of cell fragments devoid of chromatin (cytoplast) (Fig. 3k, l).

We further examined the cell division phenotypes by analysing spindle morphology after mRNA knockdown. We observed severe spindle defects for 23 genes displaying different aberrations (Table 1). The RNAi phenotype of 20 genes showed spindles with two or more microtubule foci and a reduced number of microtubule connections between the foci and the chromosomes (Fig. 3d–h), indicating a defect in microtubule assembly and/or the centrosome cycle. For seven genes displaying mitotic arrest upon mRNA knockdown, we observed no obvious spindle defects, indicating that a different primary defect must be associated with the mitotic arrest.

The knockdown of *KIF11* (Fig. 3b) and the nuclear RNA helicase

©2004 Nature Publishing Group

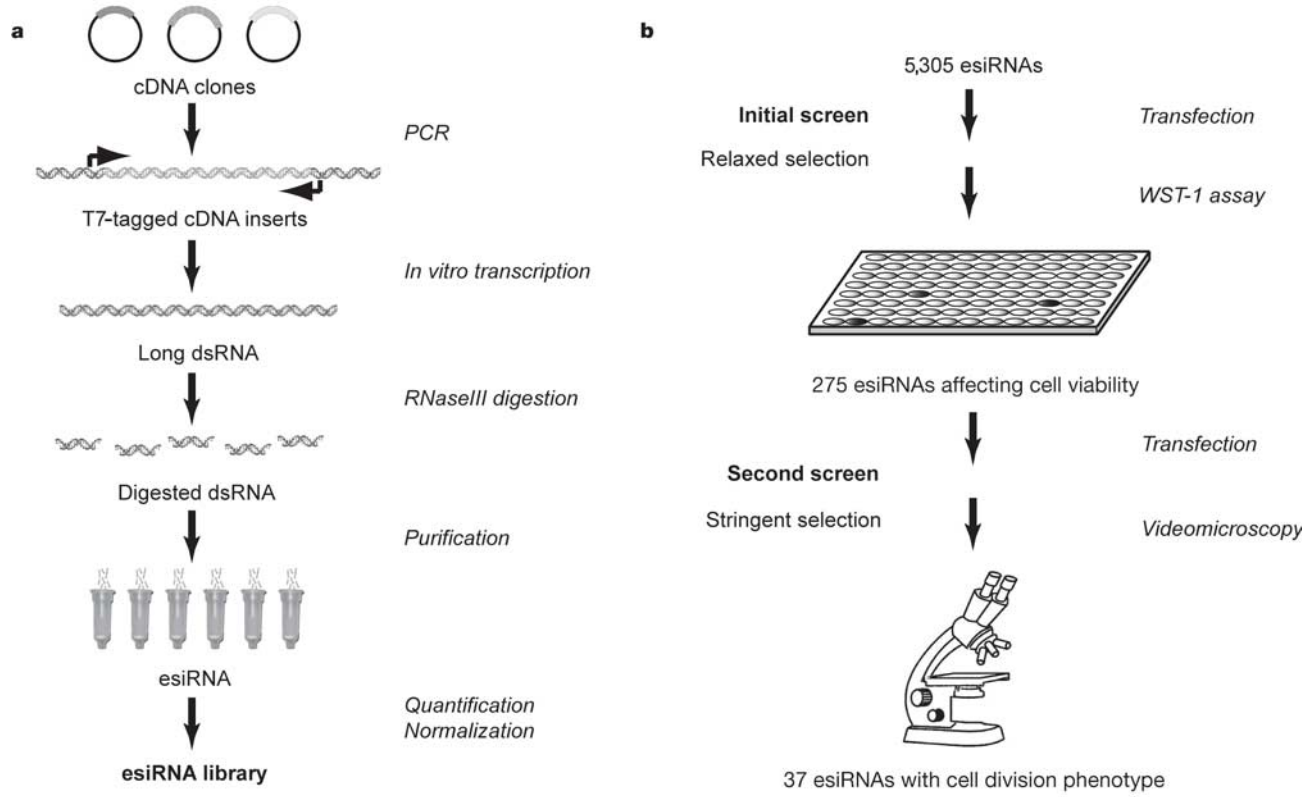

Figure 1 Library generation and screening strategy. **a**, Scheme for the generation of a large-scale esiRNA library. All steps were done in 96-well plates. **b**, Strategy for screening genes essential for cell division. Important steps are shown in italic.

Table 1 **Thirty-seven genes essential for cell division in human cells**

Gene	Functional annotation	Mitotic arrest	Cytokinesis defect	Death*	Spindle
CDC16	APC/C subunit	Yes	No	No	Abnormal
CDC27	APC/C subunit	Yes	No	No	Abnormal
CENPE	Motor protein	Yes	No	No	Normal
KIF11	Motor protein	Yes	No	No	Abnormal
KIAA0056	Condensin subunit	Yes	Yes	No	Abnormal
AD024	Kinetochore protein	Yes	Yes	No	Abnormal
RRM2	Ribonucleotide reductase	No	No	Yes	Abnormal
GALNT5	Glycosyl transferase	Yes	Yes	No	Normal
CKLFSF4	Cytokine	No	Yes	No	Normal
HRI	Protein kinase	Yes	No	No	Abnormal
ITPR1	Receptor protein	No	Yes	No	Normal
PSCD3	Receptor protein	Yes	No	No	Normal
CASP8AP2	Apoptosis factor	No	No	Yes	Normal
DDX5	Splicing factor	Yes	No	No	Abnormal
DHX8	Splicing factor	Yes	Yes	No	Abnormal
LSM6	Splicing factor	Yes	No	No	Abnormal
SART1	Splicing factor	Yes	No	No	Abnormal
SNRPA1	Splicing factor	Yes	Yes	No	Abnormal
SNRPB	Splicing factor	Yes	Yes	No	Abnormal
SNW1	Splicing factor	Yes	Yes	No	Abnormal
MFAP1	Microfibril component	Yes	Yes	No	Abnormal
ZDHHC5	Transcription factor	Yes	No	No	Normal
DDX48	Translation factor	Yes	No	No	Abnormal
EIF3S3	Translation factor	No	No	Yes	Unclear
EIF3S10	Translation factor	No	No	Yes	Unclear
CLDN16	Structural protein	Yes	No	No	Abnormal
KPNB1 (importin-β)	Importin	Yes	Yes	No	Abnormal
VCP (*p97*)	Vesicular transport protein	Yes	No	No	Abnormal
AP1S1	Vesicular transport protein	Yes	No	No	Normal
ATP6V1D	Vacuolar ATPase	Yes	No	No	Normal
DKFZP564M082	Unknown	Yes	No	No	Abnormal
FLJ10290	Unknown	Yes	Yes	No	Unclear
FLJ20311	Unknown	Yes	No	No	Abnormal
FLJ30851	Unknown	Yes	No	No	Abnormal
MGC3248	Unknown	Yes	No	No	Normal
FLJ38663	Unknown	No	No	Yes	Abnormal
MGC2603	Unknown	No	No	Yes	Normal

*Cell death upon entry into mitosis.

©2004 Nature Publishing Group

DDX48 (Fig. 3c) resulted in monopolar spindles. *KIF11* is a kinesin-like motor protein that is required for centrosome separation and therefore the establishment of a bipolar spindle[20,21]. For RNAi of importin-β we observed many rounded-up cells with apparently uncondensed chromatin and a level of microtubule nucleation consistent with interphase (Fig. 3i). Thus, although the cell cortex displays the characteristics of a mitotic cell, the presence of uncondensed chromatin suggests that these cells are in interphase. Because importin-β is a key component of Ran-dependent nuclear protein import[22], the RNAi phenotype suggests that importin-β is required for the import of proteins that trigger the progression of the nucleus from interphase into mitosis.

Surprisingly, many genes that displayed cell division phenotypes with spindle defects are known components of the splicing machinery, including *SNRPA1*, *SNRPB*, *SNW1*, *DHX8*, *DDX5*, *LSM6* and *SART1*. In principle, there are two possible explanations for this phenomenon. The simplest explanation would be that the cell division defect is an indirect consequence of defects in pre-mRNA splicing. In this scenario, the depletion of splicing factors leads to impaired pre-mRNA processing of genes essential for cell division processes, in turn resulting in depletion of the corresponding protein(s). This has been shown for the temperature-sensitive yeast splicing factors *PRP16*, *PRP19* and *Cef1*, which impair α-tubulin synthesis thereby preventing spindle assembly[23,24]. According to this scenario, the knockdown of splicing factors precedes the depletion of gene(s) essential for cell division, and impaired mitosis is a resulting secondary effect.

Alternatively, some splicing factors might have a direct role in cell division. Several points indicate that this might be the case. First, an indirect effect of splicing factors on cell division would imply that the turnover rate of these proteins and the subsequent depletion of mitosis-specific gene(s) has to be fast. However, it has recently been reported that most splicing factors have a low turnover rate[25]. Because all spliceosome RNAi phenotypes became visible 36–48 h after transfection, it is difficult to imagine that the subsequent depletion of mitosis-specific gene(s) would be fast enough and sufficient to explain the cell division phenotypes. Second, in the yeast experiments mentioned above, a marked reduction of α-tubulin levels was noted upon inactivation of spliceosome subunits[23,24]. In contrast, our tubulin stainings did not show a detectable change in α-tubulin levels (Fig. 3). Third, nuclear run-on experiments of several splicing factor knockdowns showed that general transcription, and therefore splicing, is not affected (data not shown). Fourth, *TPX2*, which is required for chromosome-induced microtubule assembly during spindle formation[26], has recently been shown to co-purify with spliceosome components[27]. Interestingly, the spindle defect observed upon *TPX2* depletion by RNAi resembles the phenotype observed here with some splicing factors; this supports the idea of a direct link between splicing and cell division. In this context it is worth mentioning that knockdown of *MFAP1*, an extracellular matrix component of the elastin-associated microfibrils, results in a cell division phenotype similar to that observed with the splicing factors in our study; mass spectrometry also showed *MFAP1* to be a component of the spliceosome[27]. Future studies will be required to determine whether the observed cell division defects result from direct or indirect interactions between splicing factors and the spindle assembly machinery.

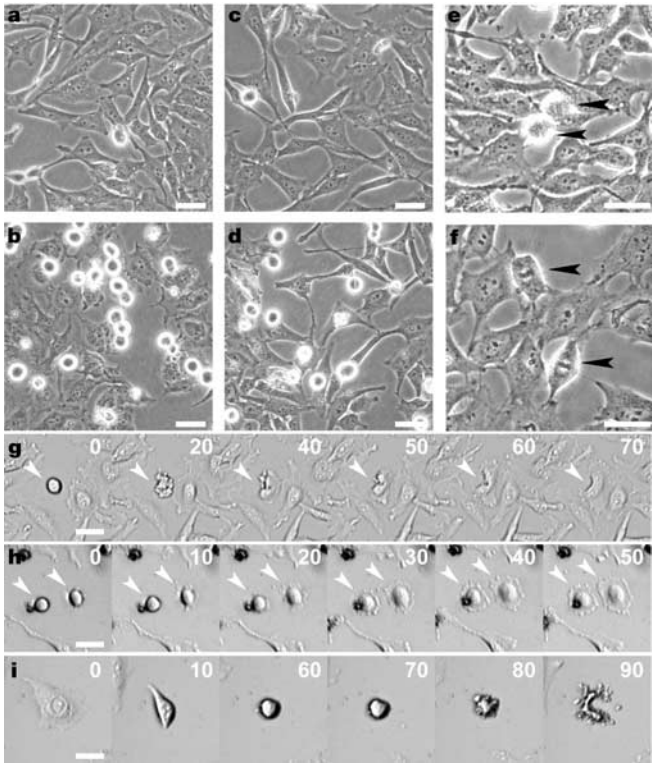

Figure 2 Cell division phenotypes visualized by videomicroscopy. **a**–**i**, HeLa cells were transfected with esiRNA targeting *SNW1* (**b**), FLJ30851 (**d**), KIAA1387 (**f**), firefly luciferase (negative control, **a**, **c**, **e**), *GALNT5* (**g**), *SNRPA1* (**h**) or *RRM2* (**i**). Microscopic images were taken after 48 h (**a**, **b**, **c**, **d**) or 72 h (**e** and **f**). The arrows indicate cells in metaphase (**e**), the KIAA1387-knockdown phenotype (**f**) and cells with cytokinesis defects (**g**, **h**). The arrows in **g** indicate the generation of two nuclei in a single cell. Numbers indicate minutes after the start of the time-lapse sequence. Scale bars are 40 μm.

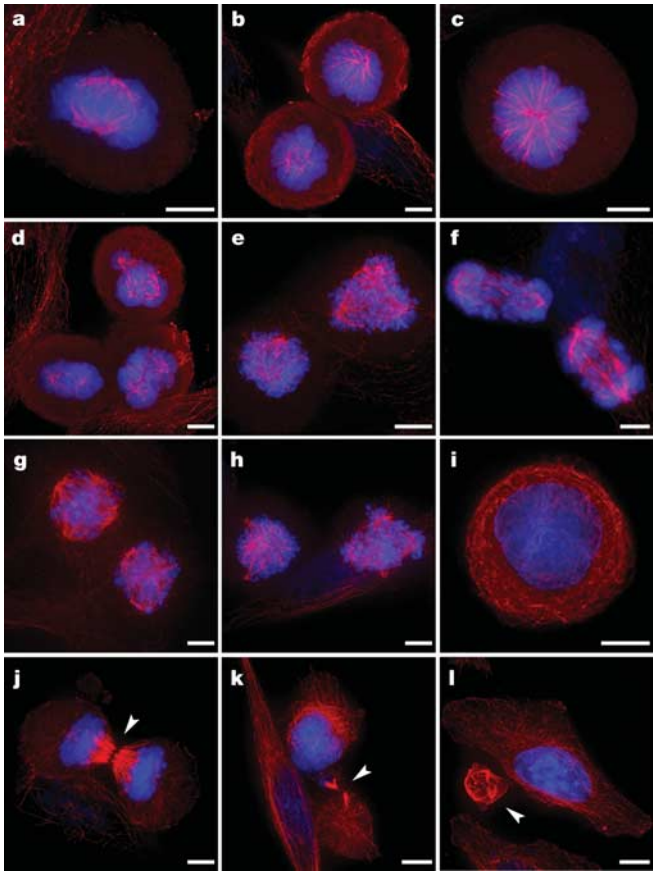

Figure 3 Spindle and cytokinesis defects observed for RNAi phenotypes. **a**–**l**, HeLa cells were transfected with esiRNA targeting firefly luciferase (negative control, **a**, **j**), *KIF11* (**b**), *DDX48* (**c**), *SNW1* (**d**, **l**), *DHX8* (**e**, **k**), *MFAP1* (**f**), DKFZP564M082 (**g**), FLJ30851 (**h**), importin-β (**i**) and imaged by three-dimensional deconvolution microscopy 48 h after transfection. Cells were stained for tubulin (red) and DNA (blue). Scale bars are 5 μm. The arrows in **j** and **k** indicate the position of the cleavage furrow. The arrow in **l** points to the collapsed cytoplast.

©2004 Nature Publishing Group

Another unexpected finding of this study was the identification of a gene for which knockdown increases cell growth rate. So far, loss-of-function leading to an increase in cell growth has only been identified for a very small number of genes. One such gene, *P27KIP1*, opposes mitotic stimuli and therefore has a negative regulatory role on cell proliferation[28]. Consistent with this, RNAi of *P27KIP1* resulted in a significantly increased growth rate in our screen (data not shown). For another gene in this class (KIAA1387), we observed a remarkable cell division phenotype of continuous cellular attachment during mitosis (Fig. 2f). The partial detachment or 'rounding-up' of the cell during mitosis is a general feature of many epithelial cells, although the reason for this morphological change is not clear. In addition, cells with RNAi for KIAA1387 also progressed significantly faster through mitosis with a transit time of 26 ± 7 min compared to 36 ± 8 min for control cells. Because the complete sequence of human KIAA1387 was not known, we cloned and sequenced this gene from cDNA, and identified two splice variants in HeLa cells. Using green fluorescent protein (GFP) fusion constructs, we determined that KIAA1387 localizes to the nucleus (see Supplementary Fig. 2a–d). Bioinformatic analyses suggest that KIAA1387 contains a Ran-binding domain, a DUF625 domain (of unknown function) and ARM (armadillo) repeat domains (see Supplementary Fig. 2e). On the basis of these analyses, we postulate that KIAA1387 is a nuclear, Ran-binding protein implicated in nuclear–cytoplasmic transport processes (see Supplementary Information). Studies are currently underway to investigate how this role results in the observed phenotype.

Crucial parameters for RNAi screens are the efficiency and specificity with which each gene is silenced. In order to test the efficiency of our screen we performed three analyses. First, we chose two multi-protein complexes, the 20S (core) proteasome and the ribosome, and identified which of their subunit genes were present in the esiRNA library after the cell viability screen. As both of these complexes are essential, knockdown of these proteins should have an effect in the cell viability assay. A similar strategy was recently used to validate an shRNA library, which identified five out of twelve core subunits essential for proteasome function[15]. In our study, nine out of nine proteasome core subunits (Fig. 4a) and 23 out of 26 ribosomal proteins (see Supplementary Table 2 and Supplementary Fig. 3) were identified using the cell viability assay. Importantly, the three remaining ribosomal genes either were not expressed in HeLa cells (the Y-chromosome-specific isologue *RPS4Y*) or are retroposons, which are dispensible for ribosomal structure and function (Fig. 4b). Therefore, we detected all of the genes from these protein complexes that are essential for growth and viability. Second, we compared published data on RNAi-mediated cell division phenotypes in tissue culture cells with our data set. We found 26 publications reporting 32 cell division defects upon mRNA knockdown. Of these, 11 genes were present in our esiRNA library, and nine of these were reported to result in reduced cell viability (see Supplementary Table 3). Six of these nine genes were picked up in our cell viability assay. Third, the percentage of essential genes detected by our screen in HeLa cells is almost identical to that reported recently for *Drosophila melanogaster* tissue culture cells[8]. Further analysis revealed that in our esiRNA library, 71.8% of the human orthologues to essential fruitfly genes were also found to be essential for cell viability in HeLa cells (see Supplementary Information). This probably reflects conservation of fundamental biological processes between fly and human cells, and indicates that the esiRNA screen in HeLa cells was similarly efficient to the screen in *Drosophila* cells.

In order to evaluate the specificity of esiRNA in our experiments, we first analysed the set of ribosomal genes in more detail. The three ribosomal genes that were not identified in the screen share 79–89% DNA sequence similarity to genes that were identified (*RPS4X*/*RPS4Y*, *RPL12*/*RPL12*-like, *RPL10*/*RPL10*-like), suggesting that esiRNA is highly target-specific. This was further confirmed by quantification of *RPS4X* knockdown after transfection of esiRNAs specific for *RPS4X* and *RPS4Y*, which are 82% identical (Fig. 4c and Supplementary Fig. 4). Second, we generated independent esiRNAs for 21 genes identified as essential for cell division, using a different region of each of the genes for esiRNA production. All of the new esiRNAs produced the same phenotype as the original esiRNAs (data not shown), suggesting a high degree of specificity for esiRNAs. This is not unexpected, because pooling of siRNAs (esiRNA represents a heterogeneous pool of siRNAs targeting the same mRNA) has been suggested to reduce off-target effects[29,30].

Our screen has uncovered additional human genes associated with cell division, thereby creating a starting point for further insight into this fundamental biological process. Our work also highlights the potential of using esiRNA in mammals to screen individual genes. The method is efficient, specific and easily adjustable to different cell-based assays, and is therefore well suited to provide insight into various aspects of mammalian biology. □

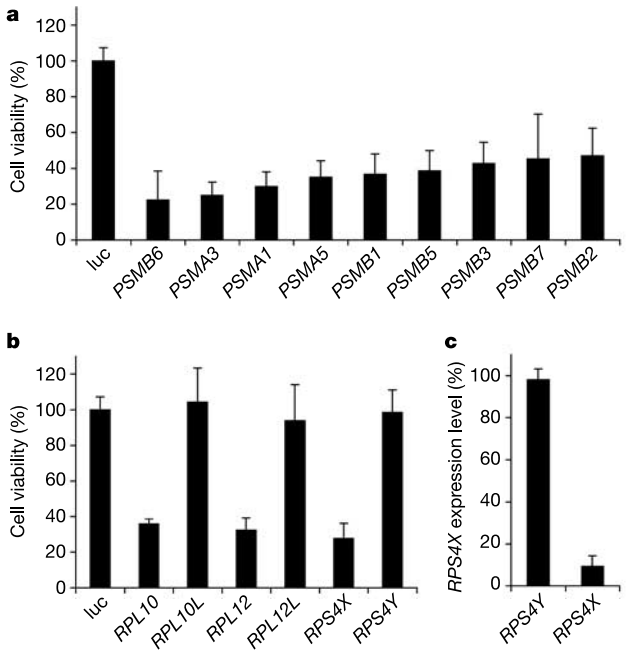

Figure 4 Efficiency and specificity of esiRNA. **a**, Effect on cell viability of esiRNAs targeting nine different subunits of the 20S proteasome. **b**, Effect on cell viability of three esiRNAs targeting essential ribosomal proteins (*RPL10*, *RPL12* and *RPS4X*) and their paralogues (*RPL10L*, *RPL12L* and *RPS4Y*). Cells in **a** and **b** were assayed 72 h after transfection. Cell viability was normalized against control esiRNA transfected cells (esiRNA directed against firefly luciferase, luc). **c**, *RPS4X* mRNA expression after transfection of esiRNAs targeting *RPS4X* and *RPS4Y* (see also Supplementary Fig. 4). All error bars represent s.d.

Methods

Generation of the esiRNA library

We generated a library from cDNA clones of the Human Ensembl Set, which were obtained from the German Genome Resource Center (RZPD). These clones have been sequence-verified in order to ensure correct annotation. One advantage of using the Ensembl Set is that these clones are derived from inserts with a length of 500–1,200 base pairs (bp), close to the 3′ end of the transcript. This avoids highly conserved or repetitive sequences (the Ensembl Set was originally created for the production of spot arrays for gene expression analyses). This clone set is well suited to the synthesis of esiRNAs because the exclusion of highly conserved sequences reduces the risk of cross-silencing homologous genes. Detailed protocols for tagging cDNA clone inserts with T7 promoter sequences (using PCR), *in vitro* transcription, digestion of long dsRNA and purification of esiRNA can be found in the Supplementary Information. Details on esiRNA library generation can also be found at http://www.mpi-cbg.de/esiRNA.

Cell-based RNAi screen

HeLa cells were seeded 16 h before transfection into 96-well plates at a density of 1,200 cells

©2004 Nature Publishing Group

per well in 100 μl medium (DMEM, 10% FBS, 2 mM L-glutamine, 100 U ml^{-1} penicillin, 100 μg ml^{-1} streptomycin). Transfections were performed in triplicate using 25 ng esiRNA and oligofectamine (Invitrogen). Cell viability was measured 72 h after transfection using the WST-1 assay (Roche Diagnostics) with a DigiScan 400 microplate reader (ASYS) at 450 nm, using 620 nm as the reference wavelength. The background was subtracted from the absorption readings and the values were mean-centred for each 96-well plate. In the initial screen we typically selected all genes for which a normalized value greater than 1.645 s.d. or less than −1.645 s.d. was obtained at least twice. These cutoff values represent 10% of all outliers, assuming a normal distribution of values. For all positive hits we re-synthesized esiRNA starting from the original cDNA clones, which were re-sequenced and confirmed by BLAST search against the published sequence of the human genome.

We re-arrayed the esiRNAs for the proteasome core subunits, all 26 cytosolic ribosomal proteins and negative controls on a 96-well plate. Transfection and WST-1 assay were performed as described above.

Time-lapse microscopic assay

For the secondary screen we re-arrayed the esiRNAs that scored in the first screen with three negative controls (esiRNA targeting firefly luciferase) per 96-well plate. We examined all 275 genes using time-lapse bright-field microscopy, capturing one frame every 10 min over 48 h, starting 30 h after transfection. This was done with an Axiovert 200 microscope −(Zeiss), using a 5 × objective with an integrated automatic stage and incubator using METAMORPH software. We quantified the frequency of cells in mitosis for all arrest phenotypes (Supplementary Fig. 1) by counting an average of 200 cells at three different time points (frame 1, frame 150 and frame 251). For KIAA1387 and the luciferase control, the average length of time in mitosis was calculated for 40 cells by counting the number of frames between entry into and exit from mitosis from frame 250 onward.

Immunofluorescence and microscopy

For visualizing the morphology of the mitotic spindle, HeLa cells that had been transfected and grown on coverslips were fixed and permeabilized in methanol at −20 °C for 8 min. Cells were washed with PBS and incubated for 10 min in PBS containing 0.2% fish skin gelatine (PBS/FSG, Sigma) to prevent nonspecific binding of antibodies. Cells were incubated for 20 min with a mouse monoclonal antibody against tubulin (DM1, Sigma) diluted to 1 μg ml^{-1} in PBS/FSG, washed in PBS, incubated in 1 μg ml^{-1} Texas-red-conjugated secondary antibodies for 20 min at 37 °C, and washed in PBS before mounting a coverslip in the presence of DAPI (1 μg ml^{-1}) to visualize chromatin. Three-dimensional data sets were acquired using a DeltaVision imaging system (Applied Precision) equipped with an Olympus IX70 microscope, a Coolsnap camera (Roper Scientific) and a × 100, 1.4 NA PlanApochromat objective. Images were computationally deconvolved using SoftWork (Applied Precision) and shown as two-dimensional projections.

Quantification of *RPS4X* expression

HeLa cells were transfected with esiRNA directed against *RPS4Y*, *RPS4X* or firefly luciferase (negative control). Cells were harvested 48 h after transfection. RNA was extracted using the RNeasy Mini Kit (Qiagen) including a DNaseI digest. cDNA was synthesized with SuperScript II reverse transcriptase (Invitrogen) using an oligo(dT) primer. *RPS4X* mRNA expression was measured by quantitative PCR using the Brilliant SYBR Green system and the Mx4000 Multiplex Quantitative PCR system (Stratagene). For *RPS4X* we used the primers (forward) 5′-CCTGGATCTTTTGACGTGGT-3′ and (reverse) 5′-TTTCCTCGGGGAAGAGAAAT-3′, and for the reference gene *B2M* (GenBank accession number NM_004048) the primers were (forward) 5′-TGACTTTGTCACAGCCCAAG-3′ and (reverse) 5′-AGCAAGCAAGCAGAATTTGG-3′. Expression levels of *RPS4X* in cells transfected with *RPS4X*- and *RPS4Y*-specific esiRNA were normalized against the expression level of cells transfected with esiRNA targeting firefly luciferase. All experiments were performed in triplicate.

Received 13 July; accepted 1 November 2004; doi:10.1038/nature03159.

1. Fire, A. *et al.* Potent and specific genetic interference by double-stranded RNA in *Caenorhabditis elegans*. *Nature* **391,** 806–811 (1998).
2. Bernstein, E., Caudy, A. A., Hammond, S. M. & Hannon, G. J. Role for a bidentate ribonuclease in the initiation step of RNA interference. *Nature* **409,** 363–366 (2001).
3. Elbashir, S. M., Lendeckel, W. & Tuschl, T. RNA interference is mediated by 21- and 22-nucleotide RNAs. *Genes Dev.* **15,** 188–200 (2001).
4. Martinez, J., Patkaniowska, A., Urlaub, H., Luhrmann, R. & Tuschl, T. Single-stranded antisense siRNAs guide target RNA cleavage in RNAi. *Cell* **110,** 563–574 (2002).
5. Gonczy, P. *et al.* Functional genomic analysis of cell division in *C. elegans* using RNAi of genes on chromosome III. *Nature* **408,** 331–336 (2000).
6. Fraser, A. G. *et al.* Functional genomic analysis of *C. elegans* chromosome I by systematic RNA interference. *Nature* **408,** 325–330 (2000).
7. Kamath, R. S. *et al.* Systematic functional analysis of the *Caenorhabditis elegans* genome using RNAi. *Nature* **421,** 231–237 (2003).
8. Boutros, M. *et al.* Genome-wide RNAi analysis of growth and viability in *Drosophila* cells. *Science* **303,** 832–835 (2004).
9. Elbashir, S. M. *et al.* Duplexes of 21-nucleotide RNAs mediate RNA interference in cultured mammalian cells. *Nature* **411,** 494–498 (2001).
10. Paddison, P. J., Caudy, A. A., Bernstein, E., Hannon, G. J. & Conklin, D. S. Short hairpin RNAs (shRNAs) induce sequence-specific silencing in mammalian cells. *Genes Dev.* **16,** 948–958 (2002).
11. Brummelkamp, T. R., Bernards, R. & Agami, R. A system for stable expression of short interfering RNAs in mammalian cells. *Science* **296,** 550–553 (2002).
12. Yang, D. *et al.* Short RNA duplexes produced by hydrolysis with *Escherichia coli* RNase III mediate effective RNA interference in mammalian cells. *Proc. Natl Acad. Sci. USA* **99,** 9942–9947 (2002).
13. Zheng, L. *et al.* An approach to genomewide screens of expressed small interfering RNAs in mammalian cells. *Proc. Natl Acad. Sci. USA* **101,** 135–140 (2004).
14. Berns, K. *et al.* A large-scale RNAi screen in human cells identifies new components of the p53 pathway. *Nature* **428,** 431–437 (2004).
15. Paddison, P. J. *et al.* A resource for large-scale RNA-interference-based screens in mammals. *Nature* **428,** 427–431 (2004).
16. Calegari, F., Haubensak, W., Yang, D., Huttner, W. B. & Buchholz, F. Tissue-specific RNA interference in postimplantation mouse embryos with endoribonuclease-prepared short interfering RNA. *Proc. Natl Acad. Sci. USA* **99,** 14236–14240 (2002).
17. Kronke, J. *et al.* Alternative approaches for efficient inhibition of hepatitis C virus RNA replication by small interfering RNAs. *J. Virol.* **78,** 3436–3446 (2004).
18. Henschel, A., Buchholz, F. & Habermann, B. DEQOR: a web-based tool for the design and quality control of siRNAs. *Nucleic Acids Res.* **32,** W113–W120 (2004).
19. Liebel, U., Kindler, B. & Pepperkok, R. 'Harvester': a fast meta search engine of human protein resources. *Bioinformatics* **20,** 1962–1963 (2004).
20. Blangy, A. *et al.* Phosphorylation by p34cdc2 regulates spindle association of human Eg5, a kinesin-related motor essential for bipolar spindle formation *in vivo*. *Cell* **83,** 1159–1169 (1995).
21. Harborth, J., Elbashir, S. M., Bechert, K., Tuschl, T. & Weber, K. Identification of essential genes in cultured mammalian cells using small interfering RNAs. *J. Cell Sci.* **114,** 4557–4565 (2001).
22. Weis, K. Regulating access to the genome: nucleocytoplasmic transport throughout the cell cycle. *Cell* **112,** 441–451 (2003).
23. Biggins, S., Bhalla, N., Chang, A., Smith, D. L. & Murray, A. W. Genes involved in sister chromatid separation and segregation in the budding yeast *Saccharomyces cerevisiae*. *Genetics* **159,** 453–470 (2001).
24. Burns, C. G. *et al.* Removal of a single alpha-tubulin gene intron suppresses cell cycle arrest phenotypes of splicing factor mutations in *Saccharomyces cerevisiae*. *Mol. Cell. Biol.* **22,** 801–815 (2002).
25. Prasanth, K. V., Sacco-Bubulya, P. A., Prasanth, S. G. & Spector, D. L. Sequential entry of components of the gene expression machinery into daughter nuclei. *Mol. Biol. Cell* **14,** 1043–1057 (2003).
26. Gruss, O. J. *et al.* Chromosome-induced microtubule assembly mediated by TPX2 is required for spindle formation in HeLa cells. *Nature Cell Biol.* **4,** 871–879 (2002).
27. Makarov, E. M. *et al.* Small nuclear ribonucleoprotein remodeling during catalytic activation of the spliceosome. *Science* **298,** 2205–2208 (2002).
28. Sherr, C. J. & Roberts, J. M. Inhibitors of mammalian G1 cyclin-dependent kinases. *Genes Dev.* **9,** 1149–1163 (1995).
29. Dorsett, Y. & Tuschl, T. siRNAs: applications in functional genomics and potential as therapeutics. *Nature Rev. Drug Discov.* **3,** 318–329 (2004).
30. Jackson, A. L. *et al.* Expression profiling reveals off-target gene regulation by RNAi. *Nature Biotechnol.* **21,** 635–637 (2003).

Supplementary Information accompanies the paper on **www.nature.com/nature**.

Acknowledgements We thank F. Stewart, I. Baines, T. Hyman and M. Slabicki for critical reading and comments on the manuscript. We thank K. Weis for helpful discussions. We are grateful to M. Boutros for providing protein accession numbers and sequences of the cell viability screen in *Drosophila* cells. This study was supported by the Max Planck Society and by the EU-FP6 grant Mitocheck. L.P. is supported by a postdoctoral fellowship from the HFSP.

Competing interests statement The authors declare that they have no competing financial interests.

Correspondence and requests for materials should be addressed to F.B. (buchholz@mpi-cbg.de).
The sequences of KIAA1387 are deposited in GenBank under accession numbers AY825268 and AY825269.

Retinoblastoma promotes definitive erythropoiesis by repressing Id2 in fetal liver macrophages

Antonio Iavarone[1,2,3], Emerson R. King[1], Xu-Ming Dai[6], Gustavo Leone[5], E. Richard Stanley[6] & Anna Lasorella[1,2,4]

[1]*Institute for Cancer Genetics, Department of* [2]*Pathology,* [3]*Neurology and* [4]*Pediatrics, College of Physicians and Surgeons of Columbia University, New York, New York 10032, USA*
[5]*Human Cancer Genetics Program, Department of Molecular Virology, Immunology and Medical Genetics, The Ohio State University, Columbus, Ohio 43210, USA*
[6]*Department of Developmental and Molecular Biology, Albert Einstein College of Medicine, Bronx, New York 10461, USA*

In mammals, the fetal liver is the first site of definitive erythropoiesis—the generation of mature, enucleated red cells. The functional unit for definitive erythropoiesis is the erythroblastic island, a multicellular structure composed of a central macrophage surrounded by erythroblasts at various stages of differen-

©2004 Nature Publishing Group